Human Molecular Genetics, 2011, Vol. 20, No. 19 **3831–3840**
doi:10.1093/hmg/ddr304
Advance Access published on July 12, 2011

N88S seipin mutant transgenic mice develop features of seipinopathy/BSCL2-related motor neuron disease via endoplasmic reticulum stress

Takuya Yagi[1], Daisuke Ito[1,*], Yoshihiro Nihei[1], Tadayuki Ishihara[2] and Norihiro Suzuki[1]

[1]Department of Neurology, School of Medicine, Keio University, 35 Shinanomachi, Shinjuku-ku, Tokyo 160-8582, Japan and [2]Department of Neurology, National Hakone Hospital, Kazamatsuri, Odawara, Kanagawa, Japan

Received April 2, 2011; Revised June 17, 2011; Accepted July 7, 2011

Heterozygosity for mutations (N88S and P90L) in the N-glycosylation site of seipin/BSCL2 is associated with the autosomal dominant motor neuron diseases, spastic paraplegia 17 and distal hereditary motor neuropathy type V, referred to as 'seipinopathies'. Previous *in vitro* studies have shown that seipinopathy-linked mutations result in accumulation of unfolded proteins in the endoplasmic reticulum (ER), leading to the unfolded protein response and cell death, suggesting that seipinopathies is closely associated with ER stress. To further understand the molecular pathogenesis of seipinopathies, we generated a transgenic (tg) mouse line expressing the human N88S seipin mutant with the murine Thy-1 promoter to permit analyses of *in vivo* phenotypic changes. The N88S seipin tg mice develop a progressive spastic motor deficit, reactive gliosis in the spinal cord and neurogenic muscular atrophy, recapitulating the symptomatic and pathological phenotype in patients of seipinopathy. We also found that expression of mutant seipin in mice upregulated the ER stress marker, immunoglobulin-heavy-chain-binding protein, protein disulfide isomerase and X-box binding protein 1, but was not linked to significant neuronal loss in affected tissue, thereby indicating that ER stress is sufficient, while neuronal death is not necessary, for the development of motor phenotypes of seipinopathies. Our findings in the mutant seipin tg mouse provide clues to understand the relationship with ER stress and neurodegeneration, and the seipin tg mouse is a valid tool for the development of novel therapeutic strategies against ER stress-related diseases.

INTRODUCTION

The *Seipin/BSCL2* gene was originally identified as a loss-of-function gene for a rare autosomal recessive disease, congenital generalized lipodystrophy type 2 (CGL2), which is associated with severe lipoatrophy, insulin resistance, hypertriglyceridemia and mental retardation (1). A recent study demonstrated that seipin knock-out mice, which exhibit reduced adipose tissue mass, hepatic steatosis, glucose intolerance and hyperinsulinemia, recapitulate the clinical features of CGL2, thereby indicating a crucial role of seipin in adipocyte development and metabolism (2). Whereas gain-of-toxic-function mutations in the N-glycosylation site of seipin (namely, the N88S and S90L mutations) cause the autosomal dominant motor neuron disease, spastic paraplegia 17 (3), clinical phenotypes of heterozygosity for these mutations inhabit a wide spectrum, including Silver syndrome, some variants of Charcot-Marie-Tooth disease type 2, distal hereditary motor neuropathy type V and spastic paraplegia, in which upper and lower motor neurons are variously affected (4,5). As a result, currently, seipin-related motor neuron diseases are collectively referred to as 'seipinopathies' (6).

Seipin, an endoplasmic reticulum (ER)-resident membrane protein, is an N-glycosylated protein that is proteolytically cleaved into N- and C-terminal fragments and is polyubiquitinated (7). We recently showed that the N88S and S90L mutations disrupt the N-glycosylation motif, enhance ubiquitination, form inclusion bodies and appear to result in proteins that are improperly folded, leading to aberrant accumulation of the mutant protein in the ER, consequently ER stress. We also showed that expression of mutants in cultured cells activates unfolded protein response (UPR), which is a cellular stress response related to the ER stress, and induces cell

*To whom correspondence should be addressed. Tel: +81 353633788; Fax: +81 333531272; Email: d-ito@jk9.so-net.ne.jp

death, suggesting that seipinopathies are closely associated with ER stress (7,8).

Recent studies have implicated ER stress, in the form of enhanced UPR branch activity, in many neurodegenerative diseases. However, there is no direct evidence in *in vivo* models that ER stress alone can lead to neurodegeneration, and some critics have suggested that ER stress may not be central to the mechanism of neurodegeneration but rather play a minor role among the complicated degeneration processes (9).

Because it is well established that an inhibition of N-glycosylation, such as exposure to the xenotoxic agent tunicamycin, leads to accumulation of unfolded proteins in the ER and induces ER stress, it is suggested that ER stress is a key process in the pathogenesis of seipinopathies, in which both the N88S and S90L mutations disrupt N-glycosylation domain. Therefore, we proposed that seipinopathies should be considered representative of ER stress-associated neurodegenerative diseases, and studying the pathophysiology of this disorder may lead to important new insights into therapeutic approaches against ER stress-associated diseases.

From this perspective, we generated a transgenic (tg) mouse line expressing the human N88S seipin mutant under a well-established neuron-specific promoter, Thy-1 (10–12). Mutant seipin tg mice develop progressive phenotypes of disturbance to upper and lower motor neurons, which recapitulates key clinical features of seipinopathies. Remarkably, motor phenotype was associated with the formation of neuron-specific inclusion bodies and upregulation of the ER stress markers in affected neuronal tissue, supporting previous *in vitro* findings (6,8). Surprisingly, we were unable to find any evidence of neuronal cell loss in the affected regions. These results suggest that *in vivo* expression of mutant seipin leads to age-dependent motor neuron disease phenotypes reminiscent of seipinopathies, via ER stress without neuronal death, and therefore can be used to study the pathological and molecular mechanism underlying ER stress-associated neurodegeneration.

RESULTS

Generation of transgenic mouse expressing human mutant seipin

To investigate whether expression of mutant seipin protein could be a cause for the generation of the neurological phenotype observed in seipinopathy patients, the neuron-specific, murine Thy-1 promoter was used to drive expression of the human N88S seipin mutant tagged with Myc and V5-His in the central nervous system (Fig. 1A). We identified one line of N88S mutant seipin transgenic mice (N88S Tg mice) that expressed substantial levels of mutant seipin, a high-molecular weight complex and an approximately 74 kDa band, as described in a previous paper (8) (Fig. 1B and Supplementary Material, Fig. S1). Immunoblotting with an anti-Myc antibody, 9E10, demonstrated that the expression of exogenous mutant seipin is specific to the brain of N88S Tg mice (Fig. 1B). Because no anti-seipin antibody that can distinguish between mouse seipin and human seipin is available, we also analyzed the gene expression levels of endogenous mouse seipin and exogenous human seipin mRNA in the brains of non-tg mice

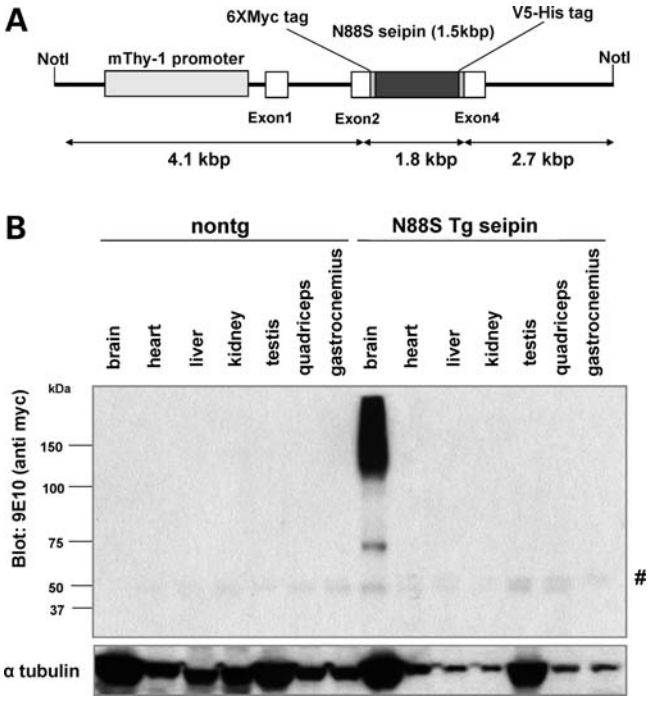

Figure 1. Expression of the N88S seipin mutant in mice. (**A**) Schematic view of the N88S seipin mutant transgene construct. The microinjected fragment was composed of the murine Thy-1 promoter and the full-length human N88S seipin mutant containing an N-terminal 6X Myc tag and a C-terminal V5-His tag. (**B**) Western blot analysis of tissue lysates using the mouse anti-Myc tag antibody, 9E10, in non-tg and N88S Tg mice. The expression of mutant seipin is specifically detected in the brain of N88S Tg mice. The pound sign (#) indicates unknown non-specific bands that reacted with the anti-Myc antibody.

and N88S Tg mice by quantitative reverse transcriptase-polymerase chain reaction (Supplementary Material, Fig. S2). The results showed no significant difference in mouse endogenous seipin expression between non-tg mice and N88S Tg mice [mRNA copy number per μg RNA: non-tg ($n = 3$) 270.6 ± 79.4, N88S Tg ($n = 3$) 252.6 ± 99.7]. Although the levels of each of the translated proteins remain unknown, the level of expression of the human transgene in N88S Tg mice [copy number per μg RNA: human transgene seipin ($n = 3$) 1727.2 ± 1004.5] was ~7-fold greater than the level of expression of the endogenous mouse seipin gene.

Progressive motor impairment in N88S Tg mice

During backcrossing with wild-type C57BL/6 strain, N88S Tg mice were born at normal Mendelian ratios, weighed the same as non-tg littermates and appeared normal in behavior. However, unstable walking and tremor-like movement were demonstrated as early symptoms in N88S Tg mice, and they become increasingly severe with age. N88S Tg mice with early onset developed motor impairment at the age of 8 weeks, and finally, all mice harboring the mutant seipin transgene developed motor symptoms by the age of 28 weeks (Supplementary Material, Videos S1 and S2). Immunoblotting of mutant seipin, using anti-Myc antibody, showed variable expression possibly due to the effect of a transitional genetic background during the backcrossing process. Notably, the

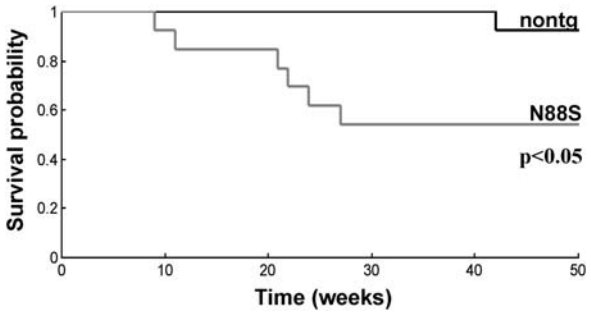

Figure 2. Kaplan–Meier survival analysis of non-tg and N88S Tg mice ($n = 13$ for each). The statistical significance was calculated using the log-rank test.

levels of mutant seipin expression are directly correlated to the onset of motor symptoms (Supplementary Material, Fig. S1). The lifespan of N88S Tg mice was significantly shorter than that of non-tg mice (Fig. 2); however, almost half of N88S Tg mice survived for more than 1 year. The body weight of N88S Tg mice was significantly lower than that of non-tg mice from 28 weeks of age onward (Fig. 3A). We did not observe any gender differences in age of onset or lifespan.

N88S Tg mice developed an abnormal hindlimb reflex characterized by retraction of the hind legs upon lifting by the tail, whereas non-tg mouse showed normal extension of the legs (Fig. 3B). N88S Tg mice began to exhibit this pathological reflex from 8 weeks of age and all N88S Tg mice displayed this reflex by 28 weeks and throughout the remainder of their lifespans (Fig. 3C). Abnormal limb reflex is a measure of motor impairment and corresponds to the spasticity occurring in human upper motor neuron disease (12–15). Therefore, this indicates that N88S Tg mice developed a spastic motor phenotype due to upper motor neuron disturbance. We have also assessed the motor functions of broods of N88S Tg mice. We performed the accelerating rotarod test and the hanging wire test every 4 weeks. The results of the accelerating rotarod test indicated progressive motor impairment, which was prominent by 24 weeks (Fig. 3D). The hanging wire test also showed that motor strength of N88S Tg mice became progressively weaker from the age of about 16 weeks (Fig. 3E). Gait abnormality was also examined by the footprint test (Supplementary Material, Fig. S3). Footprints of N88S Tg mice displayed irregularly spaced shorter strides and an uneven left–right step pattern in comparison with the evenly spaced and accurately positioned footprints of non-tg mice. At the end-stage, tg mice were unable to hold their bodies off the ground and developed a swimming-like gait, as they became severely paralyzed in their limbs and dragged them to get forward on their stomachs (Supplementary Material, Fig. S4 and Video S3). Thus, N88S Tg mice develop a spastic motor phenotype reminiscent of seipinopathies.

Inclusion bodies are formed in cerebral cortex and spinal cord of the N88S Tg mice

Previous *in vitro* studies demonstrated that expression of mutant seipin leads to the formation of unique cytoplasmic inclusion bodies, which occurs via a mechanism distinct from the formation of ubiquitinated inclusions, so-called aggresomes (7,8). To assess inclusion body formation in the brain and spinal cord of N88S Tg mice, we performed immunofluorescent histological studies. As shown in Figure 3, staining with anti-Myc antibody revealed the strong expression of exogenous N88S seipin throughout the brain and spinal cord and also cytoplasmic inclusion body formation in neuron-specific nuclear protein (NeuN)-positive neurons (Fig. 4A–C). Surprisingly, counting NeuN-positive cells showed no evidence of neuronal loss in the brain or the spinal cord, even in N88S Tg mice with advanced motor dysfunction. The number of NeuN-positive neurons was 1242 ± 139 versus 1239 ± 75 per mm^2 (in the motor cortex layer V of non-tg versus N88S Tg mice, $n = 3$) and 581 ± 61 versus 589 ± 46 per mm^2 (in anterior horn of cervical spinal cord of non-tg versus N88S Tg mice, $n = 3$). We also assessed TdT-mediated dUTP-biotin nick-end labeling, active caspase-3 and Fluro-Jade-C staining to identify cell death or neuronal degeneration, but the results showed no significant neuronal death or neuronal degeneration in N88S Tg mice (data not shown). Therefore, these findings implied that neuronal dysfunction induced by expression of mutant seipin leads to a motor phenotype in the absence of neuronal death.

Pathological analysis of N88S Tg mice

Astrocytic activation is one of the common pathological features in mouse models of motor neuron disease, such as the SOD1 and TDP-43 tg mouse models of amyotrophic lateral sclerosis (ALS) (12,13,16–19). Immunohistochemistry with anti-glial fibrillary acidic protein (GFAP) revealed pronounced reactive astrocytosis in the spinal cord of N88S Tg mice, compared with non-tg mice (Fig. 5A). Higher magnification imaging demonstrated severe gliosis in the corticospinal tract (CST) emanating from upper motor neurons in the cervical spinal cord in N88S Tg mice (Fig. 5B; 13). These pathological findings and the abnormal limb reflex shown in Figure 3B and C strongly indicated the existence of upper motor neuron disturbances in N88S Tg mice.

To assess the skeletal muscle pathology in N88S Tg mice, we performed hematoxylin and eosin staining on quadriceps femoris muscle of non-tg mice and N88S Tg mice (Fig. 5C). Skeletal muscle histology from N88S Tg mice showed typical neurogenic group atrophy, indicating lower motor neuron disturbances and/or axonopathy in N88S Tg mice. NADH-TR and ATPase staining of the skeletal muscle showed fiber-type grouping in N88S Tg mice, and provided evidence of chronic denervation (Supplementary Material, Fig. S5). Taken together, the pathological evidence and the characteristic motor deficits indicate that expression of the N88S seipin mutant in mice elicits phenotypes reminiscent of clinical features of seipinopathies due to the selective involvement of both upper and lower motor neurons.

Disruption of axonal transport in N88S Tg mice

We investigated whether the neurological dysfunction in N88S Tg mice was associated with the axon degeneration in the peripheral nerves. Histological analysis revealed severe axonal degeneration, irregular axonal morphology and dramatically increased numbers of atrophied axons in

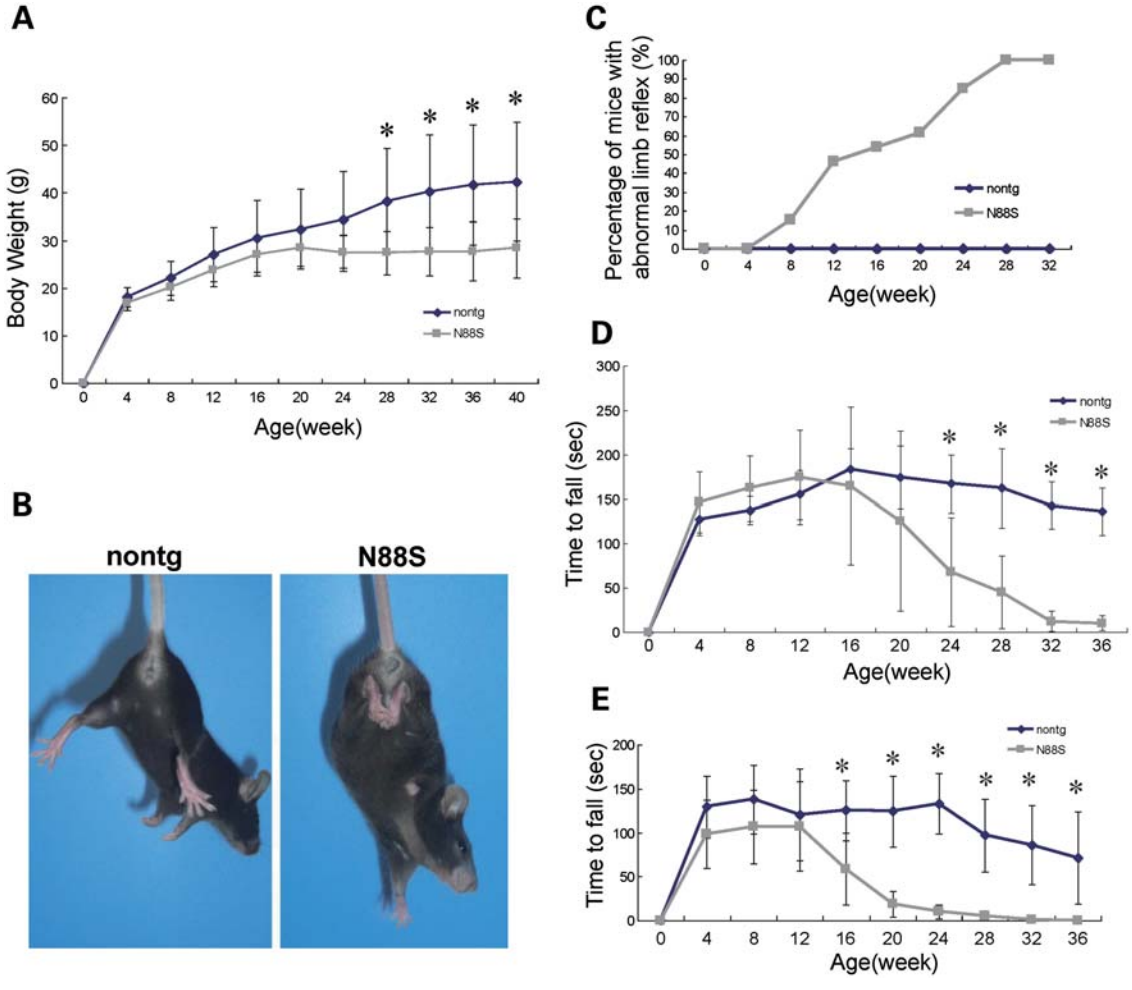

Figure 3. Neurological dysfunction in N88S Tg mice. (**A**) Body weight of non-tg and N88S Tg mice. Compared with non-tg mice, N88S Tg mice had significantly reduced body weight from 28 weeks onward. (**B**) Representative picture of abnormal limb reflexes in N88S Tg mice. Upon tail elevation, N88S Tg mice held their hindlimbs close to their body, while non-tg mice showed the normal escape response by splaying their hindlimbs. (**C**) Prevalence of abnormal limb reflex phenotype ($n = 13$). By 28 weeks, all N88S Tg mice exhibited abnormal reflexes. (**D** and **E**) Accelerating rotarod test (D) and hanging wire test (E) in non-tg and N88S Tg mice. Mice were tested every 4 weeks with the accelerating rotarod and hanging wire tests. The graphs show the falling latencies for each test. Results are expressed as means ± SD ($n = 7$). Asterisks (*) indicate a significant difference versus non-tg analyzed by Student's *t*-test ($P < 0.05$).

both the ventral roots and sciatic nerves of N88S Tg mice (Fig. 6A).

To evaluate the axonal transport in N88S Tg mice, we performed retrograde neuronal labeling by injecting the fluorescent tracer Fluoro-gold into the gastrocnemius muscle (Fig. 6B). There were significantly fewer Fluoro-gold labeled neurons in the anterior horns of the lumbar spinal cord of N88S Tg mice (20.9 ± 1.5 cells per transverse spinal cord section) than in non-tg mice (5.2 ± 1.8 cells), indicating that axonal transport was disrupted in N88S Tg mice (Fig. 6C).

Mutant seipin expression induces ER stress *in vivo*

We previously showed that expression of mutant proteins in cultured cells activates the UPR pathway, suggesting that seipinopathies are closely associated with ER stress (6,8). To verify this *in vivo*, we examined immunoblots of brain (cerebrum) lysates of three non-tg and three N88S Tg mice with antibodies against the well-established ER stress marker immunoglobulin-heavy-chain-binding protein (BiP) and protein disulfide isomerase (PDI). As shown in Figure 7A, BiP and PDI were clearly upregulated in all three N88S Tg mice. Densitometric analysis showed that expression of BiP and PDI was 3.08 ± 0.84-fold greater and 4.84 ± 0.47-fold greater, respectively, in N88S Tg mice than in non-tg mice (Fig. 7B and C). We also performed immunohistochemical studies using an anti-KDEL peptide antibody, which mainly recognized BiP, in the anterior horn of spinal cords in non-tg mice and N88S Tg mice. As shown in Figure 7D, motor neurons in the spinal cord of N88S Tg mice are stained more strongly than in non-tg mice. Moreover, immunostaining for the ER stress signaling molecule XBP1 showed the presence of X-box binding protein 1 (XBP1) positive motor neurons in the anterior horn of N88S Tg mice but not in the non-tg mice (Fig. 7E). Taken together, these findings indicated that expression of mutant seipin *in vivo* induces ER stress in affected neuronal tissue.

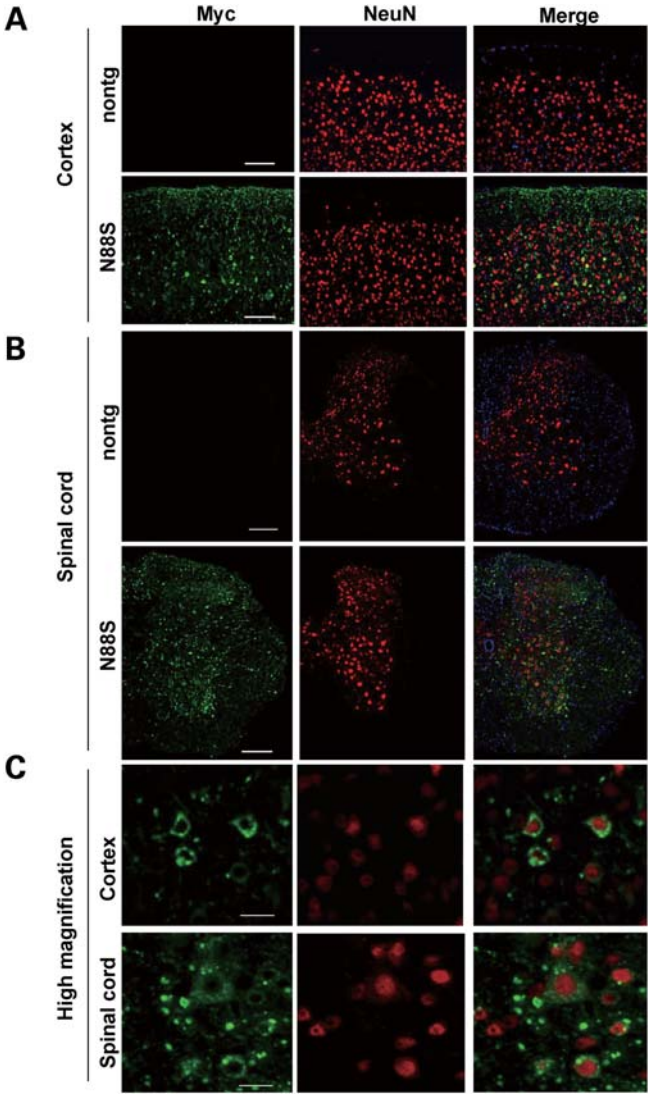

Figure 4. Immunohistological analysis of N88S Tg mouse brain and spinal cord. (**A** and **B**) Immunohistochemistry with anti-Myc (Green) and NeuN (Red) antibody in cortex (A) and spinal cord (B) from non-tg and N88S Tg mice showed expression of mutant seipin protein throughout the brain and spinal cord in N88S Tg mice. Sections were counter-stained with DAPI (Blue). Scale bar = 50 μm (A) and 250 μm (B). Note that no neuronal loss in cortical and motor neurons in the anterior horns of the spinal cords was detected. (**C**) Higher magnification images of cerebral cortex and spinal cord in N88S Tg mice showed that inclusion bodies had formed in the cytoplasm of neurons. Scale bar = 20 μm.

DISCUSSION

Mounting evidence implicates ER stress in the pathogenesis of neurodegenerative diseases, such as Alzheimer's disease, polyglutamine disease and Parkinson's disease (20–22). Recent studies of autopsy samples from patients with the most common motor neuron disease, ALS, have demonstrated the up-regulation of UPR molecules in spinal cord motor neurons, suggesting that ER stress-related neurotoxicity may be critical in the pathogenesis of ALS (23). However, it is known that the pathogenesis of most neurodegenerative diseases is known to involve extensive cross-talk between various molecular/neurotoxic processes, and it is difficult to study the pathological contribution of ER stress in isolation from such heterogeneous neurodegenerative processes. Therefore, it has remained unclear whether or not ER stress plays a major role in neurodegeneration, and whether ER stress alone can lead to neurodegeneration is still debated.

It is well established that proteins with impaired N-glycosylation are misfolded and accumulate in the ER, resulting in ER stress. Since previous *in vitro* evidence demonstrated that disruption of N-glycosylation sites on mutant seipin induce ER stress-associated cell death (6,8), ER stress may play an independent and/or central role in the neurodegenerative process of seipinopathies, and we have considered the seipinopathies to be a crucial disease for clarifying the relationship between ER stress and neurodegenerative disease. To examine the association of ER stress and seipinopathies in an *in vivo* study, we generated and characterized tg mice expressing the N88S seipin mutant under the control of a neuron-specific promoter. As expected, these tg mice exhibited key aspects of seipinopathies, including progressive and targeted motor impairments, and provide several insights into ER stress-associated neurodegeneration. First, N88S Tg mice developed age-dependent impairment of both upper and lower motor neurons, recapitulating clinical aspects of seipinopathies, which covers a broad spectrum of clinical phenotypes as a result of their effects on upper and lower motor neurons (Figs 3, 5 and 6). To the best of our knowledge, this is the first study to generate a mouse model of seipinopathies. The results of this study indicate that the cellular and molecular mechanisms for selective vulnerability in seipinopathies are common to both mice and humans, and that these tg mice will be a valuable tool in understanding motor neuron diseases with dual disturbance of upper and lower neurons. Another important point is that expression of the N88S seipin mutant in mice leads to the upregulation of the ER stress markers BiP, PDI and XBP1, thereby verifying that the pathological process of these diseases is closely associated with ER stress. Remarkably, no neuronal loss was detected in the brain or spinal cord of N88S Tg mice, indicating that neuronal death is unnecessary for the development of the seipinopathy phenotype to develop in mice (Fig. 4). Recent studies have revealed that UPR plays a dual role, acting as an adaptive response critical for cell survival and activating key processes mediating cell death in situations where protein misfolding defects are not corrected (24–26). Indeed, we detected the upregulation of ER chaperones, BiP and PDI, both of which have a cytoprotective role that prevents damage induced by ER stress (27,28) (Fig. 7), but they did not reveal any evidence of another ER stress marker, pro-apoptotic transcription factor C/EBP homologous protein, which is known to be linked to ER-stress-associated cell death in immunohistochemistry and immunoblot (data not shown), suggesting that ER stress in tg mice remains within the range of adaptation, but does not advance to cell death cascade stage. Importantly, as shown in Figure 6, tg mice also exhibited a severe disturbance of axonal transport. Because growing evidence shows that deficits in axonal transport directly lead to motor phenotype in early stage (29,30), we propose that ER stress, even within adaptive limits, can lead to neuronal disturbances, possibly linked to such processes as disturbance of axonal transport,

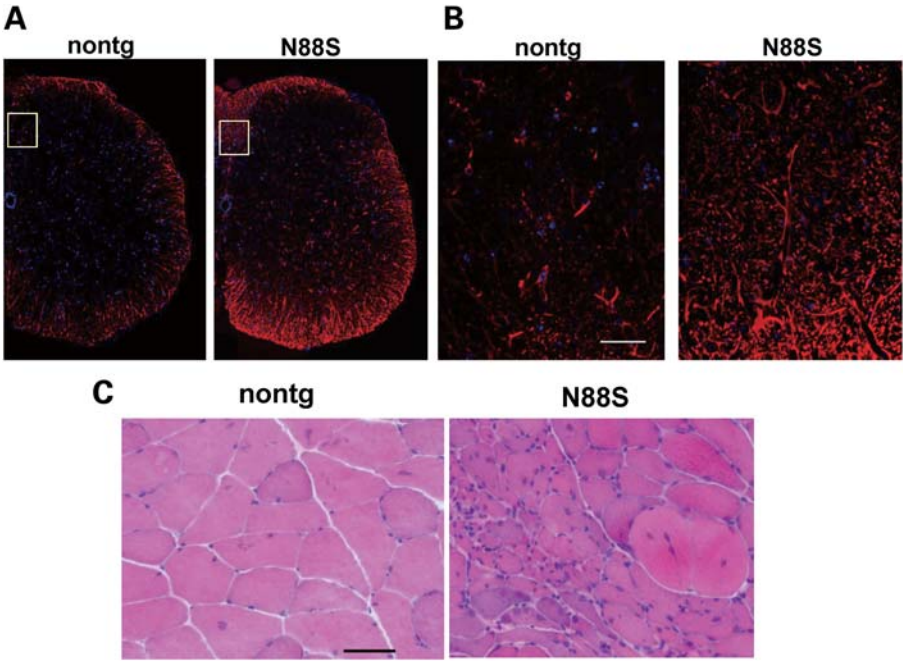

Figure 5. Reactive astrogliosis in the spinal cord of N88S Tg mice and neurogenic muscle atrophy. (**A**) Immunohistochemistry with anti-GFAP antibody (Red) in cervical spinal cords showed reactive gliosis in N88S Tg mice. (**B**) Higher magnification of CST (ventral portion of the dorsal columns: inserts in A) in cervical spinal cords of non-tg and N88S Tg mice stained with anti-GFAP antibody. Sections were counterstained with DAPI (Blue). (**C**) Hematoxylin and eosin staining of skeletal muscle (quadriceps femoris) from non-tg and N88S Tg mice at age of 50 weeks. Showing typical grouped muscle fiber atrophy in N88S Tg mice. Scale bar = 50 μm.

and that it is sufficient to cause dramatic neurological phenotypes without apparent neuronal death.

When interpreting the results of the present study, several points should be kept in mind. First, since we did not investigate whether a comparable phenotype would be observed at a similar level of overexpression of the wild-type seipin cDNA, we were unable to rule out the possibility that forced expression of seipin affected neuronal function in N88S Tg mice. Recently, tg mice with overexpression of wild-type TDP-43 as well as mice expressing an ALS-associated mutant have been reported to show pathologies associated with motor neuron degeneration reminiscent of ALS (12,13,16–18,31,32). Therefore, it is possible that forced expression of molecules, even wild-type, critical to the regulation of motor neurons, may lead to motor neuron dysfunction. Therefore, generation of a tg mouse harboring a similar level of wild-type seipin and/or a knock-in study will be needed to address these issues. However, the evidence of ER stress and inclusion formation in motor neurons in the N88S Tg mice strongly implies that the motor phenotypes are related to unfolded mutant seipin protein, and it has important implications for understanding ER stress in neurological diseases.

Secondly, because the histological analysis in the present study is limited to 40-week-old and younger tg mice, it should be examined whether long-lived N88S tg mice eventually show neuronal loss in upper and/or motor neuronal tissue or not. To the best of our knowledge, no autopsy of a seipinopathy patient has been reported and very little is known about pathological findings in this disorder. Although opportunities for an autopsy of rare and non-fatal disease, seipinopathies are difficult, it is expected that future pathological analysis will clarify whether neuronal tissue from patients also show signs of ER stress with/without motor neuron loss.

The third point that needs to be kept in mind when interpreting the results of this study is that, clinically, the neurological symptoms of seipinopathies are restricted to the motor system, i.e. upper/lower motor neuron and motor axon (6), whereas the expression of the exogenous mutant seipin in the tg mice is detected in the cerebellum and basal ganglia in addition to the cerebral cortex and spinal cord, suggesting that the tg mice may exhibit not only motor symptoms, but other neurological phenotypes as well. To establish this tg mouse as a valid model for the drug evaluation, future studies should evaluate the tg mouse for the presence of other neurological disturbances, such as cerebellar ataxia and sensory disturbances and whether or not they are linked to ER stress.

Finally, our data indicate that overexpression of seipin with the N88S mutation of an N-glycosylation site in mice results in recapitulation key features of upper/motor neuron disturbance and axonopathy in seipinopathies. Age-dependent motor phenotypes are linked to ER stress, but do not require neuronal loss in affected neuronal tissue. Based on the results of a previous *in vitro* study, this tg mouse is a crucial mouse model in which ER stress plays a key role in the neurodegenerative process. Growing evidences also implicate ER stress in the pathogenesis of various common diseases, including Alzheimer disease, brain ischemia, diabetes mellitus, atherosclerosis and neoplasm (20–22,33). We anticipate that this mouse

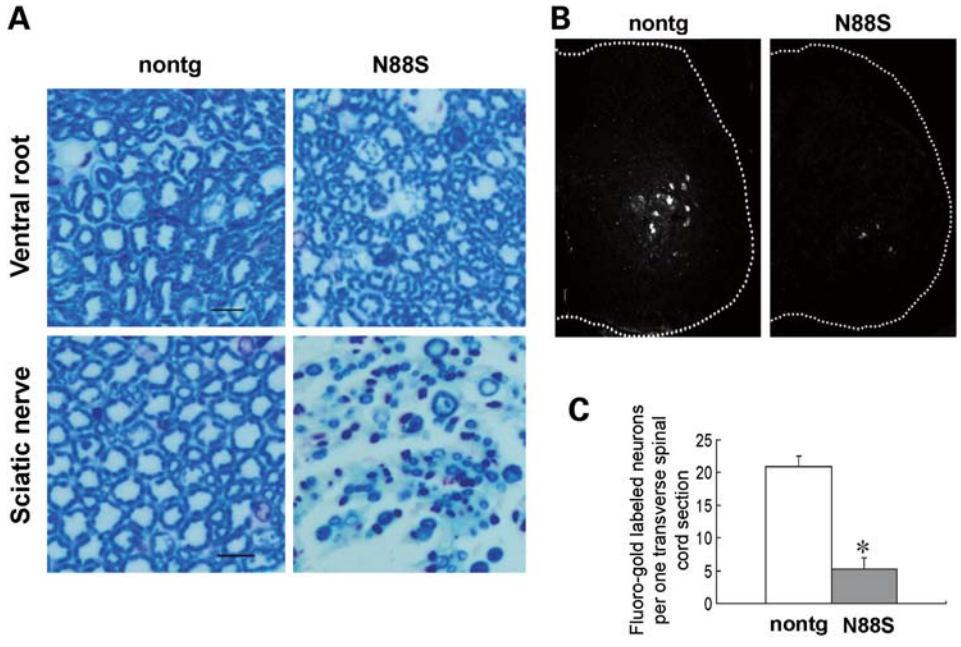

Figure 6. Dysfunction of axonal transport due to axonopathy in N88S Tg mouse. (**A**) Klüver–Barrera staining of transverse sections of ventral roots and sciatic nerves from non-tg mice and N88S Tg mice at 40 weeks of age. Note that N88S Tg mice exhibit severe axonal degeneration. Scale bar = 10 μm. (**B** and **C**) Images of transverse sections of spinal cord after retrograde labeling of lumbar motor neurons of non-tg mouse and N88S Tg mice (at 40 weeks of age) by Fluoro-gold injection of the gastrocnemius muscle (B) and the number of labeled neurons per transverse spinal cord section (C) ($n = 3$ for each). Results are expressed as means ± SD ($n = 7$). Asterisks indicate a significant difference from non-tg mice analyzed by Student's *t*-test ($P = 0.05$).

model will contribute significantly towards the understanding of the role of ER stress in neurodegeneration, as well as the development of novel therapeutic strategies against various ER stress-associated diseases.

MATERIALS AND METHODS

Generation of N88S mutant seipin transgenic mice

A human seipin cDNA with the N88S mutation was inserted into the pTSC21k vector, which encodes the 8.1 kb murine Thy1.2 expression cassette (10). This construct was *Not*I digested to remove vector sequences, purified and co-injected into the pronucleus of fertilized eggs from Slc:BDF1 strain mice. Founders were bred and backcrossed with C57Bl6/J mice to establish tg lines. Genotyping from tail DNA was performed using the following primer pairs 5′-ACAAG CTACTTGTTCTTTTTGCAG-3′ and 5′-CTAGCTGCTCTG CCACCTG-3′. All animal experiments were approved by the Ethics Committee of Keio University and conducted according to the Animal Experimentation Guidelines of Keio University School of Medicine.

Quantitative real-time PCR analysis

We prepared total RNA from mouse whole brain by the TRIzol method (Invitrogen, Carlsbad, CA, USA). The cDNA was synthesized from 1 μg RNA by using the SuperscriptIII First-Strand Synthesis System (Invitrogen). Taqman assays were designed with StepOne Software v2.0 (Applied Biosystems, Foster City, CA, USA). Expression levels of human and mouse seipin were quantified on an ABI StepOnePlus (Applied Biosystems). Taqman Rodent glyceraldehyde-3-phosphate dehydrogenase control reagents (Applied Biosystems) were used as internal control. Each sample was measured in triplicate. The primer sets used for these assays were mouse seipin (sense, 5′-GAGCCAGAGGCTAGT GATGG-3′; probe, 5′-GAAGATGCAGCTTTGCTGAC-3′; and antisense, 5′-CAAGCAGCTGCCACAAAATA-3′) and human seipin (sense, 5′-TAGAGCCTGAGGCCAGTGATG-3′; probe, 5′-GAAGATGCAGCTTTGCTGAC-3′; and antisense, 5′-GGAGAGGGTTAGGGATAGGC-3′).

Accelerating rotarod test

The accelerating rotarod apparatus (Neuroscience Inc., Tokyo, Japan) was used to analyze motor function. Mice received three trials per day for three consecutive days, allowing at least 15 min of rest between each trial. The rotating speed was accelerating gradually from 4 to 40 rpm and was maintained at 40 rpm thereafter. The mean latency to fall off the rotarod was recorded with a maximum of 360 s and used in subsequent analysis.

Hanging wire test

The mice were placed on top of a wire cage lid. The lid was shaken slightly a few times to make the mice grip the wires and then the lid was inverted. The latency to fall was recorded with a maximum of 180 s.

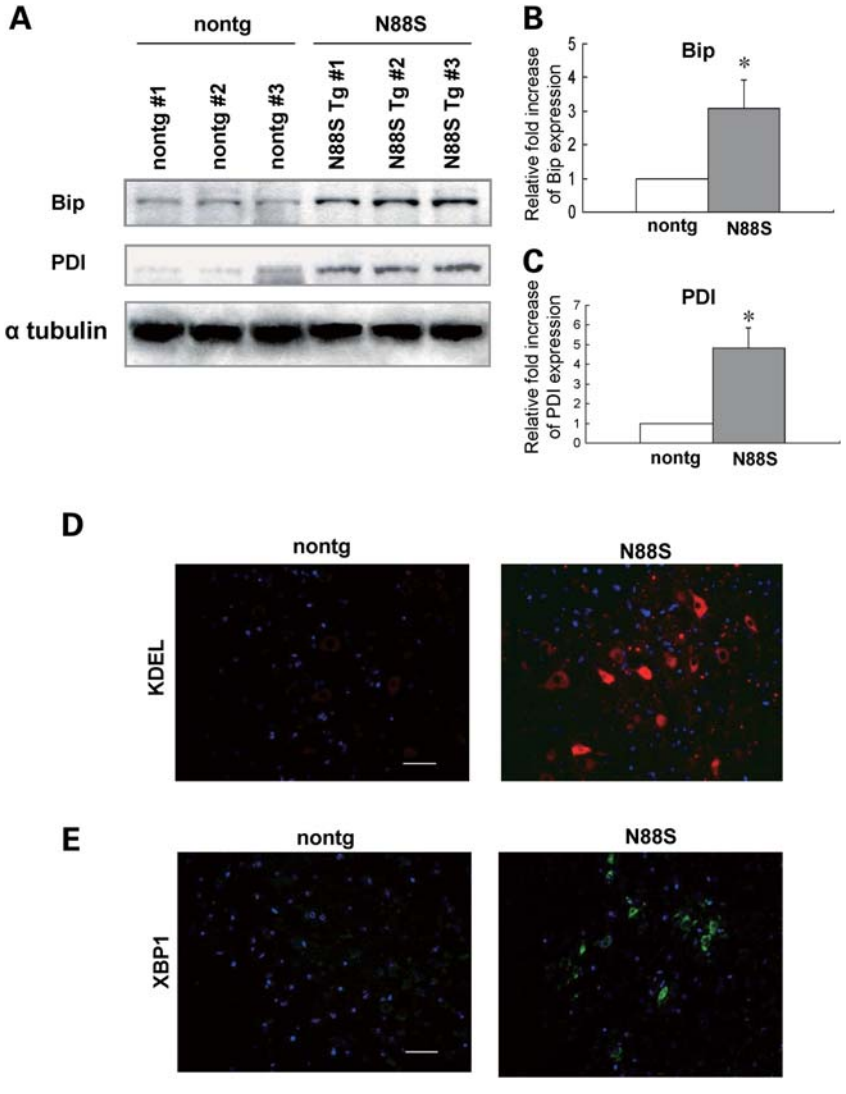

Figure 7. Induction of ER stress in N88S Tg mice. (**A**) Immunoblot analysis of the ER stress marker BiP and PDI in non-tg and N88S Tg mice ($n = 3$ for each). α-Tubulin served as an internal loading control. (**B** and **C**) Quantitative analysis of BiP (B) or PDI (C) induction. Immunoblots were scanned and analyzed by densitometry. The levels of BiP or PDI expression were normalized to the internal control α-tubulin. The histogram shows the expression of BiP relative to that of the wild-type. Asterisks indicate a significant difference versus wild-type analyzed by Student's *t*-test ($P = 0.05$). (**D**) Immunofluorescence in the anterior horn of the spinal cord in non-tg and N88S Tg mice with anti-KDEL antibody (red). Sections were counter-stained with DAPI (blue). Note that KDEL immunoreactivity is enhanced in motor neurons in the anterior horn of N88S Tg mice. Scale bar = 50 μm. (**E**) Immunofluorescence in the anterior horn of the spinal cord of non-tg and N88S Tg mice after staining with anti-XBP1 antibody (green). Sections were counterstained with DAPI (blue). Note that XBP1-stained neurons were detected in the anterior horn of the N88S Tg mice, but not of the non-tg mice. (D and E) Scale bar = 50 μm.

Footprint

Forepaws and the hindpaws were painted with non-toxic black and red ink, respectively, and the mouse was allowed to walk along a narrow corridor on a strip of white paper.

Immunoblot analysis

Brain tissue and other organs were homogenized in cold lysis buffer [50 mM Tris–HCl, pH 7.4, 150 mM NaCl, 0.5% NP-40, 0.5% sodium deoxycholate, 0.25% sodium dodecyl sulfate, 5 mM ethylenediaminetetraacetic acid and protease inhibitor cocktail from Sigma (St Louis, MO, USA)]. Total protein concentrations in the supernatants were determined using a Bio-Rad protein assay kit (Hercules, CA, USA). The proteins were then analyzed by immunoblotting as follows: protein samples were separated by reducing sodium dodecyl sulfate-polyacrylamide gel on a 4–20% Tris-glycine gradient gel (Invitrogen, Camarillo, CA, USA), and then transferred to a polyvinylidene difluoride membrane (Millipore, Bedford, MA, USA). The membranes were incubated with primary antibodies and subsequently with horseradish peroxidase-conjugated secondary antibodies. Detection was performed using enhanced chemiluminescence reagents as described by the supplier (PerkinElmer Life Sciences, Norwalk, CT, USA). The primary antibodies used in this study were: anti-Myc 9E10 (Santa Cruz Biotechnology, Santa Cruz, CA, USA), anti-KDEL (Stressgen, Victoria, Canada) and α-tubulin (Cell Signaling Technology, Beverly, MA, USA). Protein levels in Figure 7B and C were determined by densitometry using an

Epson ES-2000 scanner (Tokyo, Japan) and Image J (National Institutes of Health, Bethesda, MD, USA).

Immunohistochemical staining

Brain and spinal cord tissues were fixed by dipping with 10% formaldehyde in phosphate buffered saline (PBS) and embedded in paraffin. Sections of formalin-fixed paraffin-embedded tissues were dipped with xylene to remove paraffin, followed by dehydration in an ethanol series. The sections were then incubated with 0.05% saponin for 30 min at room temperature in preparation for immunohistochemistry. Immunohistochemistry was performed essentially as described previously (34,35) using anti-NeuN (1:1000) (Chemicon, Temecula, CA, USA), anti-Myc (1:1000) (Santa Cruz Biotechnology), anti-GFAP (1:1000) (Sigma), anti-KDEL (1:1000) (Stressgen), anti-XBP1 (1:1000) (Santa Cruz Biotechnology) and anti-PDI antibody (Enzo Life Sciences, Plymouth Meeting, PA, USA).

Retrograde Fluoro-gold neurotracer labeling

To label neurons with the tracer, a total volume of 3 μl of 4% Fluoro-gold solution (Biotium, Hayward, CA, USA) in PBS was injected directly into the gastrocnemius muscle with a 5 μl Hamilton syringe. Spinal cords were removed 3 days later, post-fixed with 4% paraformaldehyde in phosphate buffer overnight and then floated in 30% sucrose overnight. The tissues were sectioned longitudinally on a cryostat at 20 μm. The number of labeled neurons in the anterior horn was determined by counting the number in every tenth transverse spinal cord section from the entire lumbar enlargement of the spinal cord under a microscope equipped with a UV filter.

Muscle histology

Skeletal muscles were dissected fresh, immediately frozen in isopentane cooled in liquid nitrogen and cryostat sections were cut onto slides and stained with hematoxylin and eosin or NADH-TR or ATPase.

Statistical analysis

Statistical analysis of the data was performed using the Student's *t*-test and the log-rank test with JMP 8 software program (SAS Institute, Inc.).

SUPPLEMENTARY MATERIAL

Supplementary Material is available at *HMG* online.

ACKNOWLEDGEMENTS

We are grateful to Dr Herman van der Putten (Novartis Institutes for Biomedical Research, Basel, Switzerland) for providing pTSC21k.

Conflict of Interest statement. None declared.

FUNDING

This work was supported by grants from Eisai Co. Ltd (to D.I. and N.S.) and the Research Fellowship grant of the Japan Society for the Promotion of Science (to T.Y.).

REFERENCES

1. Magre, J., Delepine, M., Khallouf, E., Gedde-Dahl, T., Jr, Van Maldergem, L., Sobel, E., Papp, J., Meier, M., Megarbane, A., Bachy, A. *et al.* (2001) Identification of the gene altered in Berardinelli-Seip congenital lipodystrophy on chromosome 11q13. *Nat Genet.*, **28**, 365–370.
2. Cui, X., Wang, Y., Tang, Y., Liu, Y., Zhao, L., Deng, J., Xu, G., Peng, X., Ju, S., Liu, G. and Yang, H. (2011) Seipin ablation in mice results in severe generalized lipodystrophy. *Hum. Mol. Genet*. [Epub ahead of print].
3. Windpassinger, C., Auer-Grumbach, M., Irobi, J., Patel, H., Petek, E., Hörl, G., Malli, R., Reed, J.A., Dierick, I., Verpoorten, N. *et al.* (2004) Heterozygous missense mutations in BSCL2 are associated with distal hereditary motor neuropathy and Silver syndrome. *Nat. Genet.*, **36**, 271–276.
4. Auer-Grumbach, M., Schlotter-Weigel, B., Lochmüller, H., Strobl-Wildemann, G., Auer-Grumbach, P., Fischer, R., Offenbacher, H., Zwick, E.B., Robl, T., Hartl, G. *et al.* (2005) Phenotypes of the N88S Berardinelli-Seip congenital lipodystrophy 2 mutation. *Ann. Neurol.*, **57**, 415–424.
5. Irobi, J., Van den Bergh, P., Merlini, L., Verellen, C., Van Maldergem, L., Dierick, I., Verpoorten, N., Jordanova, A., Windpassinger, C., De Vriendt, E. *et al.* (2004) The phenotype of motor neuropathies associated with BSCL2 mutations is broader than Silver syndrome and distal HMN type V. *Brain*, **127**, 2124–2130.
6. Ito, D. and Suzuki, N. (2009) Seipinopathy: a novel endoplasmic reticulum stress-associated disease. *Brain*, **132**, 8–15.
7. Ito, D., Fujisawa, T., Iida, H. and Suzuki, N. (2008) Characterization of seipin/BSCL2, a protein associated with spastic paraplegia 17. *Neurobiol. Dis.*, **31**, 266–277.
8. Ito, D. and Suzuki, N. (2007) Molecular pathogenesis of seipin/BSCL2-related motor neuron diseases. *Ann. Neurol.*, **61**, 237–250.
9. Zhao, L. and Ackerman, S.L. (2006) Endoplasmic reticulum stress in health and disease. *Curr. Opin. Cell Biol.*, **18**, 444–452.
10. Vidal, M., Morris, R., Grosveld, F. and Spanopoulou, E. (1990) Tissue-specific control elements of the Thy-1 gene. *EMBO J.*, **9**, 833–840.
11. Moechars, D., Dewachter, I., Lorent, K., Reversé, D., Baekelandt, V., Naidu, A., Tesseur, I., Spittaels, K., Haute, C.V., Checler, F. *et al.* (1999) Early phenotypic changes in transgenic mice that overexpress different mutants of amyloid precursor protein in brain. *J. Biol. Chem.*, **274**, 6483–6492.
12. Wils, H., Kleinberger, G., Janssens, J., Pereson, S., Joris, G., Cuijt, I., Smits, V., Ceuterick-de Groote, C., Van Broeckhoven, C. and Kumar-Singh, S. (2010) TDP-43 transgenic mice develop spastic paralysis and neuronal inclusions characteristic of ALS and frontotemporal lobar degeneration. *Proc. Natl Acad. Sci. USA*, **107**, 3858–3863.
13. Igaz, L.M., Kwong, L.K., Lee, E.B., Chen-Plotkin, A., Swanson, E., Unger, T., Malunda, J., Xu, Y., Winton, M.J., Trojanowski, J.Q. *et al.* (2011) Dysregulation of the ALS-associated gene TDP-43 leads to neuronal death and degeneration in mice. *J. Clin. Invest.*, **121**, 726–738.
14. Komatsu, M., Waguri, S., Chiba, T., Murata, S., Iwata, J., Tanida, I., Ueno, T., Koike, M., Uchiyama, Y., Kominami, E. *et al.* (2006) Loss of autophagy in the central nervous system causes neurodegeneration in mice. *Nature*, **441**, 880–884.
15. Cemal, C.K., Carroll, C.J., Lawrence, L., Lowrie, M.B., Ruddle, P., Al-Mahdawi, S., King, R.H., Pook, M.A., Huxley, C. and Chamberlain, S. (2002) YAC transgenic mice carrying pathological alleles of the MJD1 locus exhibit a mild and slowly progressive cerebellar deficit. *Hum. Mol. Genet.*, **11**, 1075–1094.
16. Tsai, K.J., Yang, C.H., Fang, Y.H., Cho, K.H., Chien, W.L., Wang, W.T., Wu, T.W., Lin, C.P., Fu, W.M. and Shen, C.K. (2010) Elevated expression of TDP-43 in the forebrain of mice is sufficient to cause neurological and pathological phenotypes mimicking FTLD-U. *J. Exp. Med.*, **207**, 1661–1673.

17. Stallings, N.R., Puttaparthi, K., Luther, C.M., Burns, D.K. and Elliott, J.L. (2010) Progressive motor weakness in transgenic mice expressing human TDP-43. *Neurobiol. Dis.*, **40**, 404–414.
18. Xu, Y.F., Gendron, T.F., Zhang, Y.J., Lin, W.L., D'Alton, S., Sheng, H., Casey, M.C., Tong, J., Knight, J., Yu, X. *et al.* (2010) Wild-type human TDP-43 expression causes TDP-43 phosphorylation, mitochondrial aggregation, motor deficits, and early mortality in transgenic mice. *J. Neurosci.*, **30**, 10851–10859.
19. Feeney, S.J., McKelvie, P.A., Austin, L., Jean-Francois, M.J., Kapsa, R., Tombs, S.M. and Byrne, E. (2001) Presymptomatic motor neuron loss and reactive astrocytosis in the SOD1 mouse model of amyotrophic lateral sclerosis. *Muscle Nerve*, **24**, 1510–1519.
20. Katayama, T., Imaizumi, K., Manabe, T., Hitomi, J., Kudo, T. and Tohyama, M. (2004) Induction of neuronal death by ER stress in Alzheimer's disease. *J. Chem. Neuroanat.*, **28**, 67–78.
21. Paschen, W. and Mengesdorf, T. (2005) Endoplasmic reticulum stress response and neurodegeneration. *Cell Calcium*, **38**, 409–415.
22. Marciniak, S.J. and Ron, D. (2006) Endoplasmic reticulum stress signaling in disease. *Physiol. Rev.*, **86**, 1133–1149.
23. Ilieva, E.V., Ayala, V., Jové, M., Dalfó, E., Cacabelos, D., Povedano, M., Bellmunt, M.J., Ferrer, I., Pamplona, R. and Portero-Otín, M. (2007) Oxidative and endoplasmic reticulum stress interplay in sporadic amyotrophic lateral sclerosis. *Brain*, **130**, 3111–3123.
24. Ito, D., Walker, J.R., Thompson, C.S., Moroz, I., Lin, W., Veselits, M.L., Hakim, A.M., Fienberg, A.A. and Thinakaran, G. (2004) Characterization of stanniocalcin 2, a novel target of the mammalian unfolded protein response with cytoprotective properties. *Mol. Cell Biol.*, **24**, 9456–9469.
25. Kaufman, R.J. (1999) Stress signaling from the lumen of the endoplasmic reticulum: coordination of gene transcriptional and translational controls. *Genes Dev.*, **13**, 1211–1233.
26. Liu, C.Y. and Kaufman, R.J. (2003) The unfolded protein response. *J. Cell Sci.*, **116**, 1861–1862.
27. Rao, R.V., Peel, A., Logvinova, A., del Rio, G., Hermel, E., Yokota, T., Goldsmith, P.C., Ellerby, L.M., Ellerby, H.M. and Bredesen, D.E. (2002) Coupling endoplasmic reticulum stress to the cell death program: role of the ER chaperone GRP78. *FEBS Lett.*, **514**, 122–128.
28. Reddy, R.K., Mao, C., Baumeister, P., Austin, R.C., Kaufman, R.J. and Lee, A.S. (2003) Endoplasmic reticulum chaperone protein GRP78 protects cells from apoptosis induced by topoisomerase inhibitors: role of ATP binding site in suppression of caspase-7 activation. *J. Biol. Chem.*, **278**, 20915–20924.
29. De Vos, K.J., Grierson, A.J., Ackerley, S. and Miller, C.C. (2008) Role of axonal transport in neurodegenerative diseases. *Annu. Rev. Neurosci.*, **31**, 151–173.
30. Bilsland, L.G., Sahai, E., Kelly, G., Golding, M., Greensmith, L. and Schiavoa, G. (2010) Deficits in axonal transport precede ALS symptoms *in vivo*. *Proc. Natl Acad. Sci. USA*, **107**, 20523–20528.
31. Shan, X., Chiang, P.M., Price, D.L. and Wong, P.C. (2010) Altered distributions of Gemini of coiled bodies and mitochondria in motor neurons of TDP-43 transgenic mice. *Proc. Natl Acad. Sci. USA*, **107**, 16325–16330.
32. Wegorzewska, I., Bell, S., Cairns, N.J., Miller, T.M. and Baloh, R.H. (2009) TDP-43 mutant transgenic mice develop features of ALS and frontotemporal lobar degeneration. *Proc. Natl Acad. Sci. USA*, **106**, 18809–18814.
33. Harding, H.P. and Ron, D. (2002) Endoplasmic reticulum stress and the development of diabetes: a review. *Diabetes*, **51** (Suppl. 3), S455–S461.
34. Ito, D., Tanaka, K., Suzuki, S., Dembo, T. and Fukuuchi, Y. (2001) Enhanced expression of Iba1, ionized calcium-binding adapter molecule 1, after transient focal cerebral ischemia in rat brain. *Stroke*, **32**, 1208–1215.
35. Ito, D., Tanaka, K., Suzuki, S., Dembo, T., Kosakai, A. and Fukuuchi, Y. (2001) Up-regulation of the Ire1-mediated signaling molecule, Bip, in ischemic rat brain. *Neuroreport*, **12**, 4023–4028.